

**Threshold Resummation for the Production of Four Top Quarks at the LHC**Melissa van Beekveld<sup>1,\*</sup>, Anna Kulesza<sup>2,3,†</sup> and Laura Moreno Valero<sup>2,‡</sup><sup>1</sup>*Rudolf Peierls Centre for Theoretical Physics, Clarendon Laboratory, Parks Road, University of Oxford, Oxford OX1 3PU, United Kingdom*<sup>2</sup>*Institute for Theoretical Physics, WWU Münster, D-48149 Münster, Germany*<sup>3</sup>*Theoretical Physics Department, CERN, 1211 Geneva 23, Switzerland* (Received 7 January 2023; revised 4 October 2023; accepted 12 October 2023; published 20 November 2023)

We compute the total cross section for  $t\bar{t}t\bar{t}$  production at next-to-leading logarithmic (NLL') accuracy. This is the first time resummation is performed for a hadron-collider process with four colored particles in the final state. The calculation is matched to the next-to-leading order strong and electroweak corrections. The NLL' corrections enhance the total production rate by 15%. The size of the theoretical error due to scale variation is reduced by more than a factor of 2, bringing the theoretical error significantly below the current experimental uncertainty of the measurement.

DOI: [10.1103/PhysRevLett.131.211901](https://doi.org/10.1103/PhysRevLett.131.211901)

The production of four top quarks,  $pp \rightarrow t\bar{t}t\bar{t}$ , is one of the rarest standard model (SM) production processes currently accessible experimentally at the Large Hadron Collider (LHC). Its cross section is known to receive significant contributions in various SM extensions, hence an accurate measurement can set strong constraints on new physics models. Examples of such scenarios include supersymmetric theories, where the  $t\bar{t}t\bar{t}$  signal can be enhanced by squark and gluino decays [1,2], the production of a new heavy (pseudo)scalar boson in association with a  $t\bar{t}$  pair [3–5], or pair production of scalar gluons [6–9]. Moreover, the  $t\bar{t}t\bar{t}$  production rate is sensitive to the Yukawa coupling of the top quark, making it a useful process to further constrain the nature of Higgs-top quark interactions [10,11]. When interpreted in the framework of an effective theory, a measurement of the  $t\bar{t}t\bar{t}$  production process places strong constraints on the four-fermion operator [12–18].

The ATLAS and CMS experiments have searched for the production of  $t\bar{t}t\bar{t}$  at the LHC operating at  $\sqrt{s} = 13$  TeV [19–24]. In the latest ATLAS analysis [23] a cross section of  $\sigma_{t\bar{t}t\bar{t}} = 24 \pm 4(\text{stat})_{-4}^{+5}(\text{syst})$  fb is measured, whereas the recent combined analysis of CMS [24] reports a cross section of  $\sigma_{t\bar{t}t\bar{t}} = 17_{-5}^{+5}$  fb. Intriguingly, these values lie above the SM prediction, which is calculated at the next-to-leading order (NLO) accuracy both in the strong (QCD) and electroweak (EW) coupling [25–29], with the ATLAS measurement consistent with the SM result only within  $2\sigma$ . The NLO calculations carry a theoretical error due to scale

variation of around 25%, which is comparable with the size of the individual errors of the latest ATLAS and CMS measurements. It is therefore of crucial importance to improve the precision of the theoretical predictions for the  $t\bar{t}t\bar{t}$  production, especially having in mind that future analyses involve much larger sets of LHC data and the precision of the measurement will increase substantially.

More than 90% of the full NLO result originates from pure QCD interactions. Currently, the calculation of the next-to-next-to-leading order QCD corrections remains out of reach. However, it is possible to systematically consider a part of higher-order QCD corrections originating from multiple soft-gluon emissions. Given the very large partonic c.m. energy  $\sqrt{\hat{s}}$  needed to produce four top quarks,  $\sqrt{\hat{s}} \gtrsim 700$  GeV, the  $t\bar{t}t\bar{t}$  production at the LHC very often takes place close to production threshold, with any additional real radiation strongly suppressed. One can therefore expect that a large part of the higher-order corrections is due to soft emission and stems from the threshold region. Correspondingly, computing higher-order corrections of this type offers a promising way to improve the precision of the prediction.

Higher-order QCD corrections from soft gluon emission can be accounted for using resummation, either in direct QCD or in the soft-collinear effective-field-theory framework. The resummation program for processes involving multiple top quarks has been very successful over the recent years, leading to substantial improvements of theoretical precision for the calculation of the total production cross section for such processes, such as top-pair production [30–39] or  $t\bar{t}H/Z/W^\pm/\gamma$  [40–52]. However, in contrast to  $t\bar{t}t\bar{t}$ , these processes involve at most two colored particles in the final state. To the best of our knowledge, resummation for processes involving a higher number of colored particles has not been achieved before [53].

---

Published by the American Physical Society under the terms of the [Creative Commons Attribution 4.0 International license](https://creativecommons.org/licenses/by/4.0/). Further distribution of this work must maintain attribution to the author(s) and the published article's title, journal citation, and DOI. Funded by SCOAP<sup>3</sup>.

In this work, we perform for the first time the resummation of a process with four final-state colored particles at the Born level by applying direct QCD resummation methods in Mellin space to the process  $pp \rightarrow t\bar{t}t\bar{t}$ . The calculations are carried out at the next-to-leading logarithmic (NLL) accuracy, and take into account constant  $\mathcal{O}(\alpha_s)$  nonlogarithmic contributions that do not vanish at threshold (leading to NLL' accuracy).

*Methodology.*—Soft-gluon corrections get large at the absolute production threshold when  $\sqrt{\hat{s}}$  approaches  $M \equiv 4m_t$ , with  $m_t$  the top-quark mass. This corresponds to the limit  $\hat{\rho} \rightarrow 1$  with  $\hat{\rho} \equiv M^2/\hat{s}$ , and logarithmic behavior  $\alpha_s^n \ln(1 - \hat{\rho})^{2n}$ . The theory of  $2 \rightarrow 4$  threshold resummation builds on that for  $2 \rightarrow 2$  processes [31,57–59]. We work in Mellin space, where the hadronic cross section  $\sigma_{t\bar{t}t\bar{t}}(N)$  is the Mellin transform with respect to the variable  $\rho \equiv M^2/s$

$$\sigma_{t\bar{t}t\bar{t}}(N) = \int_0^1 d\rho \rho^{N-1} \sigma_{t\bar{t}t\bar{t}}(\rho) \quad (1)$$

of the hadronic cross section in momentum space

$$\begin{aligned} \sigma_{t\bar{t}t\bar{t}}(\rho) = & \sum_{i,j} \int_0^1 dx_1 f_i(x_1, \mu_F^2) \int_0^1 dx_2 f_j(x_2, \mu_F^2) \\ & \times \int_\rho^1 d\hat{\rho} \delta\left(\hat{\rho} - \frac{\rho}{x_1 x_2}\right) \hat{\sigma}_{ij \rightarrow t\bar{t}t\bar{t}}(\hat{\rho}). \end{aligned} \quad (2)$$

We use  $f_i$  to denote parton distribution functions (PDFs),  $\mu_F$  the factorization scale, and  $x_{1,2}$  the momentum fraction of the two colliding partons  $i, j$ . Two partonic channels contribute at leading order (LO),  $ij = \{q\bar{q}, gg\}$ . The cross section  $\hat{\sigma}_{ij \rightarrow t\bar{t}t\bar{t}}(N)$  is a perturbative function that obeys a refactorization in the soft and collinear limits into functions containing information on particular modes of dynamics. Correspondingly, one can identify a soft function  $\mathbf{S}$ , containing corrections originating from soft gluon radiation, and a collinear (jet) function for each initial-state leg  $\Delta_i$ , containing corrections from collinear gluon radiation. All terms that are nonlogarithmic in the soft-gluon limit reside in the hard function  $\mathbf{H}$ . These functions are defined at the cross section level, i.e., they include the necessary phase-space integrals. The refactorization in Mellin space takes the form

$$\begin{aligned} \hat{\sigma}_{ij \rightarrow t\bar{t}t\bar{t}}^{\text{res}}(N) = & \Delta_i(N+1) \Delta_j(N+1) \\ & \times \text{Tr}[\bar{\mathbf{S}}_{ij \rightarrow t\bar{t}t\bar{t}}(N+1) \otimes \mathbf{H}_{ij \rightarrow t\bar{t}t\bar{t}}(N)], \end{aligned} \quad (3)$$

suppressing the dependence on  $\mu_R$  and  $\mu_F$ . Jet and soft functions both capture soft-collinear enhancements, so one must subtract the overlap contributions through dividing out the eikonal jet functions  $\mathcal{J}_i$  from the soft function. This results in a new soft-collinear-subtracted soft function denoted by  $\bar{\mathbf{S}}$ , and related to the full one as

$$\bar{\mathbf{S}}(N+1) = \frac{\mathbf{S}(N+1)}{\mathcal{J}_1(N+1)\mathcal{J}_2(N+1)}. \quad (4)$$

The soft and hard functions are matrices in color space, indicated by their bold font, and color connected, indicated by the  $\otimes$  symbol. We now go over the definition of the ingredients in Eq. (3).

The hard function  $\mathbf{H}_{ij \rightarrow t\bar{t}t\bar{t}}$  obeys the perturbative expansion

$$\mathbf{H}_{ij \rightarrow t\bar{t}t\bar{t}} = \mathbf{H}_{ij \rightarrow t\bar{t}t\bar{t}}^{(0)} + \frac{\alpha_s}{\pi} \mathbf{H}_{ij \rightarrow t\bar{t}t\bar{t}}^{(1)} + \mathcal{O}(\alpha_s^2). \quad (5)$$

At the NLL accuracy we need  $\mathbf{H}_{ij \rightarrow t\bar{t}t\bar{t}}^{(0)}$ , defined as a matrix in color space with an element  $IJ$

$$\mathbf{H}_{ij \rightarrow t\bar{t}t\bar{t},IJ}^{(0)} = \frac{1}{2\hat{s}} \int_0^1 d\hat{\rho} \hat{\rho}^{N-1} \int d\Phi^B \sum_{\text{color,spin}} \mathcal{A}_I^{(0)} \mathcal{A}_J^{\dagger(0)}, \quad (6)$$

where we sum (average) over final(initial)-state color and polarization degrees of freedom. The Born phase space is denoted by  $\Phi^B$ . The object  $\mathcal{A}_I^{(0)} = \langle c_I | \mathcal{A}^{(0)} \rangle$  is the color-stripped amplitude projected to the color-vector  $c_I$ , with  $|\mathcal{A}^{(0)}\rangle$  the amplitude in the corresponding color basis, and  $\mathcal{A}_J^{(0)\dagger}$  is its complex conjugate. The full  $N$  dependence of the hard function is kept. We obtain the squared matrix elements numerically from aMC@NLO [26,60].

The coefficient  $\mathbf{H}_{ij \rightarrow t\bar{t}t\bar{t}}^{(1)}$  enters formally at next-to-next-to-leading logarithmic accuracy but can be used to supplement the NLL expressions, resulting in NLL' precision. It consists of virtual one-loop corrections,  $\mathbf{V}_{ij \rightarrow t\bar{t}t\bar{t}}^{(1)}$ , and constant terms stemming from collinear-enhanced contributions  $\mathbf{C}_{ij \rightarrow t\bar{t}t\bar{t}}^{(1)}$  that are not yet captured by the initial-state jet functions  $\Delta_i$ , i.e.,

$$\mathbf{H}_{ij \rightarrow t\bar{t}t\bar{t}}^{(1)} = \mathbf{V}_{ij \rightarrow t\bar{t}t\bar{t}}^{(1)} + \mathbf{C}_{ij \rightarrow t\bar{t}t\bar{t}}^{(1)}. \quad (7)$$

While the  $\mathbf{C}_{ij \rightarrow t\bar{t}t\bar{t}}^{(1)}$  coefficient is calculated analytically,  $\mathbf{V}_{ij \rightarrow t\bar{t}t\bar{t}}^{(1)}$  is obtained numerically using MadLoop [61–64]. The infrared pole structure of the MadLoop calculation, using FKS subtraction [65–67], matches that of our resummed calculation.

For the incoming jet functions we use the well-known expressions that can be found in, e.g., [68–70], which are a function of  $\lambda = \alpha_s b_0 \ln \bar{N}$  with  $\bar{N} \equiv Ne^{\gamma_E}$ . The soft function is given by [31,57]

$$\mathbf{S}_{ij \rightarrow t\bar{t}t\bar{t}} = \bar{\mathbf{U}}_{ij \rightarrow t\bar{t}t\bar{t}} \bar{\mathbf{S}}_{ij \rightarrow t\bar{t}t\bar{t}} \mathbf{U}_{ij \rightarrow t\bar{t}t\bar{t}}, \quad (8)$$

with the evolution matrix written as a path-ordered exponential

$$\mathbf{U}_{ij \rightarrow \bar{t}\bar{t}\bar{t}} = P \exp \left[ \frac{1}{2} \int_{\mu_R^2}^{M^2/\bar{N}^2} \frac{dq^2}{q^2} \Gamma_{ij \rightarrow \bar{t}\bar{t}\bar{t}}[\alpha_s(q^2)] \right], \quad (9)$$

and  $\Gamma_{ij \rightarrow \bar{t}\bar{t}\bar{t}}[\alpha_s(q^2)]$  the soft anomalous dimension (AD) matrix. To achieve NLL(') resummation one needs the one-loop contribution  $\Gamma_{ij \rightarrow \bar{t}\bar{t}\bar{t}}^{(1)}$  in Eq. (9). This object consists of a kinematic part and a color-mixing part, which accounts for the change in color of the hard system, i.e.,

$$\Gamma_{ij \rightarrow \bar{t}\bar{t}\bar{t},IJ}^{(1)} = \sum_{k,l=1}^6 \text{Tr} [c_I \mathbf{T}_k \cdot \mathbf{T}_l c_J^\dagger] \Gamma_{kl}, \quad (10)$$

where  $\mathbf{T}_k$  are color operators. The explicit expression for  $\Gamma_{ij \rightarrow \bar{t}\bar{t}\bar{t},IJ}^{(1)}$  depends on a choice of basis tensors represented by  $c_I$  (and  $c_J^\dagger$  for the complex conjugate) for the underlying hard scattering process  $ij \rightarrow \bar{t}\bar{t}\bar{t}$ . The kinematic part,  $\Gamma_{kl}$ , is given by the residue of the UV-divergent part of the one-loop eikonal contributions [30,71,72].

The matrix  $\tilde{\mathbf{S}}_{ij \rightarrow \bar{t}\bar{t}\bar{t}}$  in Eq. (8) represents the boundary condition for the solution of the renormalization group equation at  $\mu_R = M/\bar{N}$  from which Eq. (8) follows. Like  $\mathbf{H}$ , it obeys a perturbative expansion

$$\tilde{\mathbf{S}}_{ij \rightarrow \bar{t}\bar{t}\bar{t}} = \tilde{\mathbf{S}}_{ij \rightarrow \bar{t}\bar{t}\bar{t}}^{(0)} + \frac{\alpha_s}{\pi} \tilde{\mathbf{S}}_{ij \rightarrow \bar{t}\bar{t}\bar{t}}^{(1)} + \mathcal{O}(\alpha_s^2). \quad (11)$$

The lowest-order contribution  $\tilde{\mathbf{S}}_{ij \rightarrow \bar{t}\bar{t}\bar{t}}^{(0)}$  is given by the trace of the color basis vectors for the underlying hard process. For NLL' resummation we also need the first-order correction  $\tilde{\mathbf{S}}_{ij \rightarrow \bar{t}\bar{t}\bar{t}}^{(1)}$ , which is calculated analytically by considering the eikonal corrections to  $\tilde{\mathbf{S}}_{ij \rightarrow \bar{t}\bar{t}\bar{t}}^{(0)}$ .

The major difficulty in the resummed calculations for the  $\bar{t}\bar{t}\bar{t}$  production cross section stems from the complicated color structure of the underlying hard process, involving six colored particles. The color structure of the  $q\bar{q} \rightarrow \bar{t}\bar{t}\bar{t}$  process is

$$\mathbf{3} \otimes \bar{\mathbf{3}} = \mathbf{3} \otimes \bar{\mathbf{3}} \otimes \mathbf{3} \otimes \bar{\mathbf{3}}. \quad (12)$$

The decomposition into irreducible representations reads

$$\mathbf{1} \oplus \mathbf{8} = (2 \times \mathbf{1}) \oplus (2 \times \mathbf{8}) \oplus \mathbf{8}_S \oplus \mathbf{8}_A \oplus \mathbf{10} \oplus \bar{\mathbf{10}} \oplus \mathbf{27}. \quad (13)$$

For the  $gg$  channel we have

$$\mathbf{8} \otimes \mathbf{8} = \mathbf{3} \otimes \bar{\mathbf{3}} \otimes \mathbf{3} \otimes \bar{\mathbf{3}}, \quad (14)$$

and in terms of irreducible representations

$$\begin{aligned} & \mathbf{0} \oplus \mathbf{1} \oplus \mathbf{8}_S \oplus \mathbf{8}_A \oplus \mathbf{10} \oplus \bar{\mathbf{10}} \oplus \mathbf{27} \\ & = \mathbf{0} \oplus (2 \times \mathbf{1}) \oplus (2 \times \mathbf{8}) \oplus \mathbf{8}_S \oplus \mathbf{8}_A \oplus \mathbf{10} \oplus \bar{\mathbf{10}} \oplus \mathbf{27}. \end{aligned} \quad (15)$$

From this we infer that the  $q\bar{q}$  color space is six dimensional, whereas the  $gg$  one is 14 dimensional.

The one-loop soft AD matrices  $\Gamma_{ij \rightarrow \bar{t}\bar{t}\bar{t}}^{(1)}$  are in general not diagonal. Solving Eq. (9) in terms of standard exponential functions requires changing the color bases to  $R$  where  $\Gamma_{ij \rightarrow \bar{t}\bar{t}\bar{t},R}^{(1)}$  is diagonal [57]. We find such bases using the technique outlined in Ref. [73]. The resulting one-loop soft AD matrices for  $N_c = 3$  in the threshold limit become [74]

$$2\text{Re}[\bar{\Gamma}_{q\bar{q} \rightarrow \bar{t}\bar{t}\bar{t},R}] = \text{diag}(0, 0, -3, -3, -3, -3), \quad (16a)$$

$$\begin{aligned} 2\text{Re}[\bar{\Gamma}_{gg \rightarrow \bar{t}\bar{t}\bar{t},R}] = & \text{diag}(-8, -6, -6, -4, -3, -3, \\ & -3, -3, -3, -3, -3, -3, 0, 0). \end{aligned} \quad (16b)$$

The values above are the negative values of the quadratic Casimir invariants for the irreducible representations in which the color structure of the final state can be decomposed in SU(3). This corresponds to a physical picture where the soft gluon is only sensitive to the total color charge of a system at threshold, and constitutes a strong check of our calculations. We have verified that the virtual corrections obtained from MadLoop, rewritten in the new basis  $R$ , are consistently 0 for the base vector corresponding to a representation whose dimension is zero for  $N_c = 3$ , which is another consistency check of our work.

With this, the contribution of the soft-collinear-subtracted soft function reads

$$\bar{\mathbf{S}}_{ij \rightarrow \bar{t}\bar{t}\bar{t},R}(N) = \tilde{\mathbf{S}}_{ij \rightarrow \bar{t}\bar{t}\bar{t},R} \exp \left[ \frac{\text{Re}[\bar{\Gamma}_{ij \rightarrow \bar{t}\bar{t}\bar{t},R}^{(1)}]}{b_0 \pi} \ln(1 - 2\lambda) \right], \quad (17)$$

where  $\bar{\Gamma}_{ij \rightarrow \bar{t}\bar{t}\bar{t},R}^{(1)}$  is related to  $\Gamma_{ij \rightarrow \bar{t}\bar{t}\bar{t},R}^{(1)}$  after subtracting the soft-collinear contributions [58]. The hard function in Eq. (3) is written in the color tensor basis  $R$ .

The last step to calculate a physical cross section in momentum space involves taking the inverse Mellin transform of the  $N$ -space expression

$$\begin{aligned} \sigma_{\bar{t}\bar{t}\bar{t}}^{\text{NLO+res}}(\rho) = & \sigma_{\bar{t}\bar{t}\bar{t}}^{\text{NLO}}(\rho) \\ & + \sum_{ij} \int_{\mathcal{C}} \frac{dN}{2\pi i} \rho^{-N} f_i(N+1, \mu_F^2) f_j(N+1, \mu_F^2) \\ & \times [\hat{\sigma}_{ij \rightarrow \bar{t}\bar{t}\bar{t}}^{\text{res}}(N) - \hat{\sigma}_{ij \rightarrow \bar{t}\bar{t}\bar{t}}^{\text{res}}(N)|_{\text{NLO}}], \end{aligned} \quad (18)$$

where ‘‘res’’ denotes LL, NLL, or NLL'. To retain the full information from the perturbative calculation, we match the resummed result to the NLO fixed-order cross section

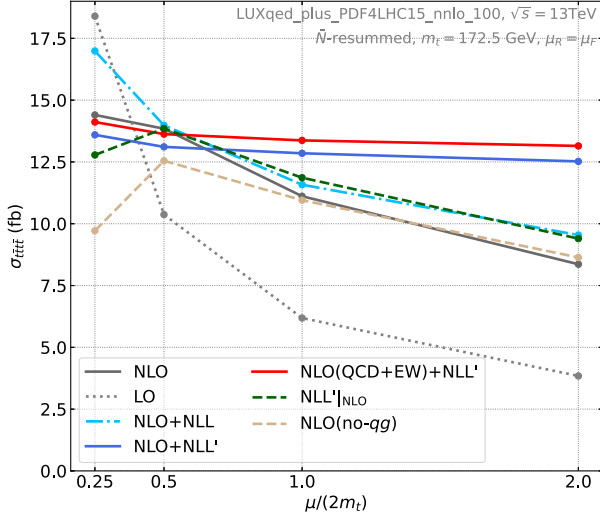


FIG. 1. Scale dependence of QCD LO (gray dotted line), NLO (gray solid line), NLO(no- $qg$ ) (brown dashed line),  $NLL'|_{NLO}$  (green dashed line), NLO + NLL (blue dash-dotted line), NLO + NLL' (blue solid line), and NLO(QCD + EW) + NLL' (red solid line) cross sections at  $\sqrt{s} = 13$  TeV.

$\sigma_{ij \rightarrow \bar{i}\bar{i}\bar{i}}^{NLO}$ . To avoid double counting, the expansion of  $\hat{\sigma}_{ij \rightarrow \bar{i}\bar{i}\bar{i}}^{\text{res}}(N)$  up to  $\mathcal{O}(\alpha_s^5)$ ,  $\hat{\sigma}_{ij \rightarrow \bar{i}\bar{i}\bar{i}}^{\text{res}}(N)|_{NLO}$ , is subtracted. The inverse Mellin transform in Eq. (18) used the minimal prescription [76] and is evaluated numerically on a contour  $\mathcal{C}$  parameterized by  $C_{MP}$  and  $\phi_{MP}$  as

$$N = C_{MP} + ye^{i\phi_{MP}}, \quad (19)$$

with  $y \in [0, \infty)$ . We calculated results for various values  $C_{MP}$  and  $\phi_{MP}$  to verify the independence of the result on the choice of the contour. Inverting the resummed expression from Mellin to physical space involves choosing a specific approach. Other methods than the minimal prescription could be used, see, e.g., [33,77]. Different methods reorganize subleading terms differently, leading to numerical differences in the predictions and thus an additional source of uncertainty.

TABLE I. Fixed and resummed-and-matched total cross sections in fb for  $pp \rightarrow \bar{i}\bar{i}\bar{i}$  with  $\sqrt{s} = 13$  TeV and  $\sqrt{s} = 13.6$  TeV, the central scale value of  $\mu_0 = 2m_t$ , and  $m_t = 172.5$  GeV. The number in parentheses indicates the statistical uncertainty on the last digit whereas the percentage error indicates the seven-point scale uncertainty [Eq. (20)]. The  $K_{NLL'}$  factor is the ratio of the resummation-improved cross section at NLO + NLL' to the NLO cross section.

$\sqrt{s}$ (TeV)	NLO	NLO + NLL	NLO + NLL'	$K_{NLL'}$
13	11.00(2) $^{+25.2\%}_{-24.5\%}$ fb	11.46(2) $^{+21.3\%}_{-17.7\%}$ fb	12.73(2) $^{+4.1\%}_{-11.8\%}$ fb	1.16
13.6	13.14(2) $^{+25.1\%}_{-24.4\%}$ fb	13.81(2) $^{+20.7\%}_{-20.1\%}$ fb	15.16(2) $^{+2.5\%}_{-11.9\%}$ fb	1.15
$\sqrt{s}$ (TeV)	NLO(QCD + EW)	NLO(QCD + EW) + NLL	NLO(QCD + EW) + NLL'	$K_{NLL'}$
13	11.64(2) $^{+23.2\%}_{-22.8\%}$ fb	12.10(2) $^{+19.5\%}_{-16.3\%}$ fb	13.37(2) $^{+3.6\%}_{-11.4\%}$ fb	1.15
13.6	13.80(2) $^{+22.6\%}_{-22.9\%}$ fb	14.47(2) $^{+18.5\%}_{-19.1\%}$ fb	15.82(2) $^{+1.5\%}_{-11.6\%}$ fb	1.15

*Numerical results.*—The phenomenological studies reported in this Letter are performed using the central member of the LUXqed\_plus\_PDF4LHC15\_nnlo\_100 PDF set [78,79] for both the pure QCD results and the QCD + EW results. This PDF set is based on the PDF4LHC15 PDF set [80–83] and includes the photon content of the proton. We use the  $\alpha_s$  value corresponding to the PDF set, take the mass of the top quark  $m_t = 172.5$  GeV (unless stated otherwise), and choose the central factorization and renormalization scale  $\mu_{F,0} = \mu_{R,0} = 2m_t$  (as in Ref. [27]). The theoretical uncertainty is estimated by varying  $\mu_R$  and  $\mu_F$  using a seven-point scale variation, i.e.,

$$\left( \frac{\mu_R}{\mu_{R,0}}, \frac{\mu_F}{\mu_{F,0}} \right)_{\text{seven point}} \in \{(0.5, 0.5), (0.5, 1), (1, 0.5), (1, 1), (1, 2), (2, 1), (2, 2)\}. \quad (20)$$

The fixed-order results are obtained using aMC@NLO [26,60]. Since our calculation concerns pure QCD corrections, we present the LO and NLO QCD results for comparison. However, our final resummation-improved cross section incorporates the NLO(QCD + EW) result, where the electroweak corrections are included up to  $\mathcal{O}(\alpha^2)$  [28,85].

Figure 1 shows the scale dependence of various fixed-order and resummed results for  $\sigma_{\bar{i}\bar{i}\bar{i}}$  setting  $\mu_R = \mu_F$ . To judge the quality of the resummation we include the expanded NLL' resummed result, and the exact NLO cross section without the  $qg$  channel, named NLO(no- $qg$ ). We observe that apart from the region of very small scales, the expanded result captures more than 90% of the NLO(no- $qg$ ) cross section [86]. While the NLL corrections only moderately improve the scale dependence of the NLO QCD cross section, the scale sensitivity of the NLO + NLL' result is dramatically reduced. NLL' contributions increase the  $\sigma_{\bar{i}\bar{i}\bar{i}}$  predictions by 16% with respect to the pure NLO QCD result, and by 15% with respect to the complete NLO(QCD + EW) result, see Table I. These corrections are more than twice the size of the previously calculated complete EW effects at NLO. Based on the

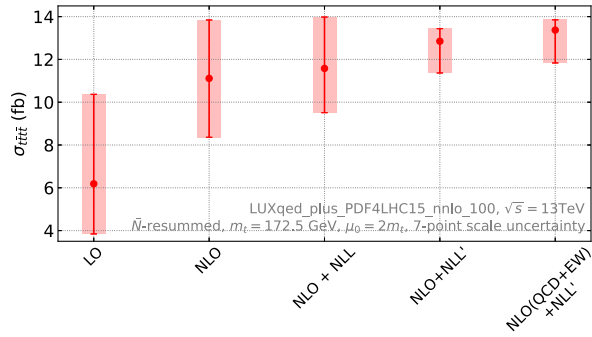


FIG. 2. Predictions for the total  $pp \rightarrow t\bar{t}t$  cross section at  $\sqrt{s} = 13$  TeV for fixed-order calculations and resummation-improved results, obtained using Eq. (20).

results presented here we expect that the central value of the NLO + NNLL predictions will be close to the NLO + NLL' result. The former calculation will, however, likely bring down the scale uncertainty of the theoretical predictions, and is left for future work.

Next we examine the reduction of the theoretical error of the resummation-improved cross section using the seven-point method. Table I summarizes the central values of the various predictions together with the corresponding error due to scale variation. This information is graphically represented in Fig. 2. Remarkably, the scale error of the NLO + NLL' predictions is reduced compared to NLO predictions by more than a factor of 2. Including the PDF uncertainty of  $\pm 6.9\%$ , our state-of-the-art prediction for  $\sqrt{s} = 13$  TeV and  $m_t = 172.5$  GeV reads

$$\sigma_{t\bar{t}t}^{\text{NLO(QCD+EW)+NLL}'} = 13.37(2)^{+0.48}_{-1.52}(\text{scale}) \pm 0.92(\text{pdf}) \text{ fb},$$

or, adding the two theoretical errors in quadrature

$$\sigma_{t\bar{t}t}^{\text{NLO(QCD+EW)+NLL}'} = 13.37(2)^{+1.04}_{-1.78} \text{ fb}. \quad (21)$$

Resumming terms logarithmic in  $N$  shifts the central value by 0.54 fb. We defer a detailed discussion to an upcoming publication [84,87]. In Table I we also report the obtained cross section for the LHC c.m. energy of 13.6 TeV. Including the scale uncertainty of  $\pm 6.7\%$  we obtain

$$\begin{aligned} \sigma_{t\bar{t}t}^{\text{NLO(QCD+EW)+NLL}'} &= 15.82(2)^{+0.24}_{-1.83}(\text{scale}) \pm 1.06(\text{pdf}) \text{ fb} \\ &= 15.82(2)^{+1.09}_{-2.11} \text{ fb}, \end{aligned}$$

which is an increase of 18.3% with respect to the obtained cross section for  $\sqrt{s} = 13$  TeV.

We have also studied the effect of varying the value of the top mass in the window of 170–175 GeV. The resulting predictions are shown in Fig. 3 for  $\sqrt{s} = 13$  TeV. We observe that the correction stemming from soft-gluon resummation is flat under variation of the top quark mass.

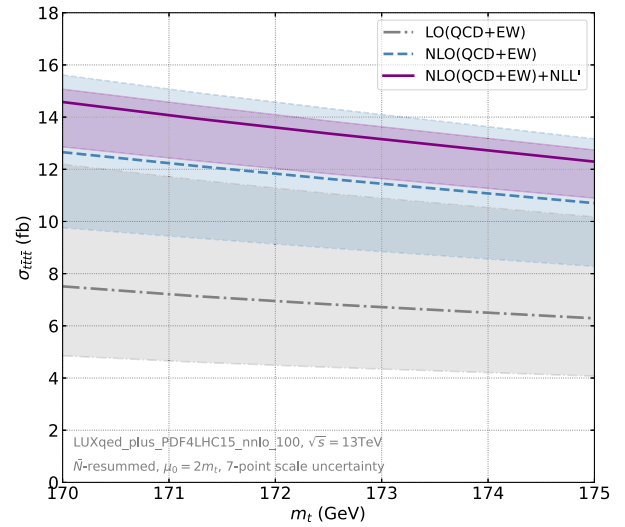


FIG. 3. Cross section for the  $pp \rightarrow t\bar{t}t$  process with  $\sqrt{s} = 13$  TeV for different values of  $m_t$ . Shown are the LO, NLO, and NLO + NLL' predictions (QCD + EW). The bands indicate the scale uncertainty calculated using Eq. (20).

*Conclusion.*—In this Letter, we present predictions for the total cross section of the four top production process at NLO + NLL' accuracy, including electroweak corrections for the fixed-order prediction. This is the first time that the framework of threshold resummation has been applied to a  $2 \rightarrow 4$  process containing six colored particles at leading order. We present our results both at a collider energy of 13 and 13.6 TeV, and vary the top mass in the window of 170–175 GeV. Setting  $m_t = 172.5$  GeV and  $\sqrt{s} = 13.6$  TeV, we find the total cross section  $\sigma_{t\bar{t}t}^{\text{NLO(QCD+EW)+NLL}'} = 15.8^{+1.5\%}_{-11.6\%}$  fb, where the indicated error is estimated using the seven-point scale uncertainty. When compared to the NLO(QCD + EW)-only prediction,  $\sigma_{t\bar{t}t}^{\text{NLO(QCD+EW)}} = 13.8^{+22.6\%}_{-22.9\%}$  fb, we find that the central value is increased with a  $K$  factor of 1.15. The uncertainty stemming from scale variation is reduced by more than a factor of two. Including the PDF error in quadrature we reduce the total theoretical uncertainty from  $(+23.6\%, -23.9\%)$  at NLO(QCD + EW) to  $(+6.8\%, -13.4\%)$  at NLO(QCD + EW) + NLL', which lies comfortably below the current experimental uncertainty. These predictions will play an important role in stress testing the SM, especially in view of the latest experimental results obtained for  $t\bar{t}t$  production.

We are grateful to Marco Zaro and Davide Pagani for their help in extracting the NLO electroweak corrections from aMC@NLO. This work has been supported in part by the DFG Grant No. KU 3103/2. M. vB. acknowledges support from a Royal Society Research Professorship (RP/R1/180112) and from the Science and Technology Facilities Council under Grant No. ST/T000864/1, while

L. M. V. acknowledges support from the DFG Research Training Group “GRK 2149: Strong and Weak Interactions —from Hadrons to Dark Matter.” A. K. gratefully acknowledges the support and the hospitality of the CERN Theoretical Physics Department.

\*melissa.vanbeekveld@physics.ox.ac.uk

†anna.kulesza@uni-muenster.de

‡l\_more02@uni-muenster.de

- [1] G. R. Farrar and P. Fayet, Phenomenology of the production, decay, and detection of new hadronic states associated with supersymmetry, *Phys. Lett.* **76B**, 575 (1978).
- [2] M. Toharia and J. D. Wells, Gluino decays with heavier scalar superpartners, *J. High Energy Phys.* **02** (2006) 015.
- [3] D. Dicus, A. Stange, and S. Willenbrock, Higgs decay to top quarks at hadron colliders, *Phys. Lett. B* **333**, 126 (1994).
- [4] N. Craig, F. D’Eramo, P. Draper, S. Thomas, and H. Zhang, The hunt for the rest of the Higgs bosons, *J. High Energy Phys.* **06** (2015) 137.
- [5] N. Craig, J. Hajer, Y.-Y. Li, T. Liu, and H. Zhang, Heavy Higgs bosons at low  $\tan\beta$ : From the LHC to 100 TeV, *J. High Energy Phys.* **01** (2017) 018.
- [6] T. Plehn and T. M. P. Tait, Seeking sgluons, *J. Phys. G* **36**, 075001 (2009).
- [7] S. Calvet, B. Fuks, P. Gris, and L. Valery, Searching for sgluons in multitop events at a center-of-mass energy of 8 TeV, *J. High Energy Phys.* **04** (2013) 043.
- [8] L. Beck, F. Blekman, D. Dobur, B. Fuks, J. Keaveney, and K. Mawatari, Probing top-philic sgluons with LHC run I data, *Phys. Lett. B* **746**, 48 (2015).
- [9] L. Darmé, B. Fuks, and M. Goodsell, Cornering sgluons with four-top-quark events, *Phys. Lett. B* **784**, 223 (2018).
- [10] Q.-H. Cao, S.-L. Chen, and Y. Liu, Probing Higgs Width and Top Quark Yukawa Coupling from  $t\bar{t}H$  and  $t\bar{t}\bar{t}$  Productions, *Phys. Rev. D* **95**, 053004 (2017).
- [11] Q.-H. Cao, S.-L. Chen, Y. Liu, R. Zhang, and Y. Zhang, Limiting top quark-Higgs boson interaction and Higgs-boson width from multitop productions, *Phys. Rev. D* **99**, 113003 (2019).
- [12] C. Zhang, Constraining  $qqtt$  operators from four-top production: A case for enhanced EFT sensitivity, *Chin. Phys. C* **42**, 023104 (2018).
- [13] G. Banelli, E. Salvioni, J. Serra, T. Theil, and A. Weiler, The present and future of four top operators, *J. High Energy Phys.* **02** (2021) 043.
- [14] D. Barducci *et al.*, Interpreting top-quark LHC measurements in the standard-model effective field theory, [arXiv:1802.07237](https://arxiv.org/abs/1802.07237).
- [15] N. P. Hartland, F. Maltoni, E. R. Nocera, J. Rojo, E. Slade, E. Vryonidou, and C. Zhang, A Monte Carlo global analysis of the Standard Model Effective Field Theory: the top quark sector, *J. High Energy Phys.* **04** (2019) 100.
- [16] J. J. Ethier, G. Magni, F. Maltoni, L. Mantani, E. R. Nocera, J. Rojo, E. Slade, E. Vryonidou, and C. Zhang (SMEFT Collaboration), Combined SMEFT interpretation of Higgs, diboson, and top quark data from the LHC, *J. High Energy Phys.* **11** (2021) 089.
- [17] L. Darmé, B. Fuks, and F. Maltoni, Top-philic heavy resonances in four-top final states and their EFT interpretation, *J. High Energy Phys.* **09** (2021) 143.
- [18] R. Aoude, H. El Faham, F. Maltoni, and E. Vryonidou, Complete SMEFT predictions for four top quark production at hadron colliders, *J. High Energy Phys.* **10** (2022) 163.
- [19] A. M. Sirunyan *et al.* (CMS Collaboration), Search for production of four top quarks in final states with same-sign or multiple leptons in proton-proton collisions at  $\sqrt{s} = 13$  TeV, *Eur. Phys. J. C* **80**, 75 (2020).
- [20] A. M. Sirunyan *et al.* (CMS Collaboration), Search for the production of four top quarks in the single-lepton and opposite-sign dilepton final states in proton-proton collisions at  $\sqrt{s} = 13$  TeV, *J. High Energy Phys.* **11** (2019) 082.
- [21] M. Aaboud *et al.* (ATLAS Collaboration), Search for four-top-quark production in the single-lepton and opposite-sign dilepton final states in pp collisions at  $\sqrt{s} = 13$  TeV with the ATLAS detector, *Phys. Rev. D* **99**, 052009 (2019).
- [22] G. Aad *et al.* (ATLAS Collaboration), Evidence for  $t\bar{t}\bar{t}$  production in the multilepton final state in proton-proton collisions at  $\sqrt{s} = 13$  TeV with the ATLAS detector, *Eur. Phys. J. C* **80**, 1085 (2020).
- [23] G. Aad *et al.* (ATLAS Collaboration), Measurement of the  $t\bar{t}\bar{t}$  production cross section in  $pp$  collisions at  $\sqrt{s} = 13$  TeV with the ATLAS detector, *J. High Energy Phys.* **11** (2021) 118.
- [24] CMS Collaboration, Evidence for the simultaneous production of four top quarks in proton-proton collisions at  $\sqrt{s} = 13$  TeV, Technical Report, CERN, Geneva, 2022.
- [25] G. Bevilacqua and M. Worek, Constraining BSM Physics at the LHC: Four top final states with NLO accuracy in perturbative QCD, *J. High Energy Phys.* **07** (2012) 111.
- [26] J. Alwall, R. Frederix, S. Frixione, V. Hirschi, F. Maltoni, O. Mattelaer, H. S. Shao, T. Stelzer, P. Torrielli, and M. Zaro, The automated computation of tree-level and next-to-leading order differential cross sections, and their matching to parton shower simulations, *J. High Energy Phys.* **07** (2014) 079.
- [27] F. Maltoni, D. Pagani, and I. Tsinikos, Associated production of a top-quark pair with vector bosons at NLO in QCD: Impact on  $t\bar{t}H$  searches at the LHC, *J. High Energy Phys.* **02** (2016) 113.
- [28] R. Frederix, D. Pagani, and M. Zaro, Large NLO corrections in  $t\bar{t}W^\pm$  and  $t\bar{t}\bar{t}$  hadroproduction from supposedly subleading EW contributions, *J. High Energy Phys.* **02** (2018) 031.
- [29] T. Ježo and M. Kraus, Hadroproduction of four top quarks in the POWHEG BOX, *Phys. Rev. D* **105**, 114024 (2022).
- [30] N. Kidonakis and G. F. Sterman, Resummation for QCD hard scattering, *Nucl. Phys.* **B505**, 321 (1997).
- [31] H. Contopanagos, E. Laenen, and G. F. Sterman, Sudakov factorization and resummation, *Nucl. Phys.* **B484**, 303 (1997).
- [32] R. Bonciani, S. Catani, M. L. Mangano, and P. Nason, NLL resummation of the heavy quark hadroproduction cross-section, *Nucl. Phys.* **B529**, 424 (1998); **B803**, 234(E) (2008).
- [33] N. Kidonakis, E. Laenen, S. Moch, and R. Vogt, Sudakov resummation and finite order expansions of heavy quark

- hadroproduction cross-sections, *Phys. Rev. D* **64**, 114001 (2001).
- [34] M. Czakon, A. Mitov, and G.F. Sterman, Threshold resummation for top-pair hadroproduction to next-to-next-to-leading log, *Phys. Rev. D* **80**, 074017 (2009).
- [35] M. Beneke, P. Falgari, and C. Schwinn, Soft radiation in heavy-particle pair production: All-order colour structure and two-loop anomalous dimension, *Nucl. Phys.* **B828**, 69 (2010).
- [36] V. Ahrens, A. Ferroglia, M. Neubert, B. D. Pecjak, and L. L. Yang, Renormalization-group improved predictions for top-quark pair production at hadron colliders, *J. High Energy Phys.* **09** (2010) 097.
- [37] M. Cacciari, M. Czakon, M. Mangano, A. Mitov, and P. Nason, Top-pair production at hadron colliders with next-to-next-to-leading logarithmic soft-gluon resummation, *Phys. Lett. B* **710**, 612 (2012).
- [38] M. Beneke, P. Falgari, S. Klein, and C. Schwinn, Hadronic top-quark pair production with NNLL threshold resummation, *Nucl. Phys.* **B855**, 695 (2012).
- [39] M. Czakon, A. Ferroglia, D. Heymes, A. Mitov, B. D. Pecjak, D. J. Scott, X. Wang, and L. L. Yang, Resummation for (boosted) top-quark pair production at NNLO + NNLL' in QCD, *J. High Energy Phys.* **05** (2018) 149.
- [40] A. Kulesza, L. Motyka, T. Stebel, and V. Theeuwes, Soft gluon resummation for associated  $t\bar{t}H$  production at the LHC, *J. High Energy Phys.* **03** (2016) 065.
- [41] A. Kulesza, L. Motyka, T. Stebel, and V. Theeuwes, Soft gluon resummation at fixed invariant mass for associated  $t\bar{t}H$  production at the LHC, *Proc. Sci. LHCP2016* (2016) 084.
- [42] A. Kulesza, L. Motyka, T. Stebel, and V. Theeuwes, Associated  $t\bar{t}H$  production at the LHC: Theoretical predictions at NLO + NNLL accuracy, *Phys. Rev. D* **97**, 114007 (2018).
- [43] A. Kulesza, L. Motyka, D. Schwartzländer, T. Stebel, and V. Theeuwes, Associated production of a top quark pair with a heavy electroweak gauge boson at NLO + NNLL accuracy, *Eur. Phys. J. C* **79**, 249 (2019).
- [44] A. Kulesza, L. Motyka, D. Schwartzländer, T. Stebel, and V. Theeuwes, Associated top quark pair production with a heavy boson: Differential cross sections at NLO + NNLL accuracy, *Eur. Phys. J. C* **80**, 428 (2020).
- [45] M. van Beekveld and W. Beenakker, The role of the threshold variable in soft-gluon resummation of the  $t\bar{t}h$  production process, *J. High Energy Phys.* **05** (2021) 196.
- [46] H. T. Li, C. S. Li, and S. A. Li, Renormalization group improved predictions for  $t\bar{t}W^\pm$  production at hadron colliders, *Phys. Rev. D* **90**, 094009 (2014).
- [47] A. Broggio, A. Ferroglia, B. D. Pecjak, A. Signer, and L. L. Yang, Associated production of a top pair and a Higgs boson beyond NLO, *J. High Energy Phys.* **03** (2016) 124.
- [48] A. Broggio, A. Ferroglia, G. Ossola, and B. D. Pecjak, Associated production of a top pair and a W boson at next-to-next-to-leading logarithmic accuracy, *J. High Energy Phys.* **09** (2016) 089.
- [49] A. Broggio, A. Ferroglia, B. D. Pecjak, and L. L. Yang, NNLL resummation for the associated production of a top pair and a Higgs boson at the LHC, *J. High Energy Phys.* **02** (2017) 126.
- [50] A. Broggio, A. Ferroglia, G. Ossola, B. D. Pecjak, and R. D. Sameshima, Associated production of a top pair and a Z boson at the LHC to NNLL accuracy, *J. High Energy Phys.* **04** (2017) 105.
- [51] A. Broggio, A. Ferroglia, R. Frederix, D. Pagani, B. D. Pecjak, and I. Tsirikos, Top-quark pair hadroproduction in association with a heavy boson at NLO + NNLL including EW corrections, *J. High Energy Phys.* **08** (2019) 039.
- [52] N. Kidonakis and A. Tonerio, Higher-order corrections in  $t\bar{t}\gamma$  cross sections, *Phys. Rev. D* **107**, 034013 (2023).
- [53] The calculation of the one-loop soft-anomalous dimension, needed for an NLL(') resummation, is performed for processes with 3 colored final-state particles, e.g., [54–56].
- [54] A. Kyrieleis and M. H. Seymour, The colour evolution of the process  $q\bar{q} \rightarrow q\bar{q}g$ , *J. High Energy Phys.* **01** (2006) 085.
- [55] M. Sjö Dahl, Color structure for soft gluon resummation: A General recipe, *J. High Energy Phys.* **09** (2009) 087.
- [56] B. Chargeishvili, M. V. Garzelli, and S.-O. Moch, One-loop soft anomalous dimension matrices for  $t\bar{t}j$  hadroproduction, [arXiv:2206.10977](https://arxiv.org/abs/2206.10977).
- [57] N. Kidonakis, G. Oderda, and G. F. Sterman, Threshold resummation for dijet cross-sections, *Nucl. Phys.* **B525**, 299 (1998).
- [58] N. Kidonakis, G. Oderda, and G. F. Sterman, Evolution of color exchange in QCD hard scattering, *Nucl. Phys.* **B531**, 365 (1998).
- [59] R. Bonciani, S. Catani, M. L. Mangano, and P. Nason, Sudakov resummation of multiparton QCD cross-sections, *Phys. Lett. B* **575**, 268 (2003).
- [60] R. Frederix, S. Frixione, V. Hirschi, D. Pagani, H. S. Shao, and M. Zaro, The automation of next-to-leading order electroweak calculations, *J. High Energy Phys.* **07** (2018) 185; **11** (2021) 085.
- [61] V. Hirschi, R. Frederix, S. Frixione, M. V. Garzelli, F. Maltoni, and R. Pittau, Automation of one-loop QCD corrections, *J. High Energy Phys.* **05** (2011) 044.
- [62] G. Ossola, C. G. Papadopoulos, and R. Pittau, CutTools: A program implementing the OPP reduction method to compute one-loop amplitudes, *J. High Energy Phys.* **03** (2008) 042.
- [63] F. Cascioli, P. Maierhofer, and S. Pozzorini, Scattering amplitudes with open loops, *Phys. Rev. Lett.* **108**, 111601 (2012).
- [64] A. Denner, S. Dittmaier, and L. Hofer, COLLIER: A fortran-based complex one-loop library in extended regularizations, *Comput. Phys. Commun.* **212**, 220 (2017).
- [65] S. Frixione, Z. Kunszt, and A. Signer, Three jet cross-sections to next-to-leading order, *Nucl. Phys.* **B467**, 399 (1996).
- [66] S. Frixione, A general approach to jet cross-sections in QCD, *Nucl. Phys.* **B507**, 295 (1997).
- [67] R. Frederix, S. Frixione, F. Maltoni, and T. Stelzer, Automation of next-to-leading order computations in QCD: The FKS subtraction, *J. High Energy Phys.* **10** (2009) 003.
- [68] S. Catani and L. Trentadue, Resummation of the QCD perturbative series for hard processes, *Nucl. Phys.* **B327**, 323 (1989).
- [69] S. Catani, M. L. Mangano, and P. Nason, Sudakov resummation for prompt photon production in hadron collisions, *J. High Energy Phys.* **07** (1998) 024.

- [70] S. Catani, D. de Florian, M. Grazzini, and P. Nason, Soft gluon resummation for Higgs boson production at hadron colliders, *J. High Energy Phys.* **07** (2003) 028.
- [71] J. Botts and G. Sterman, Hard elastic scattering in qcd: Leading behavior, *Nucl. Phys.* **B325**, 62 (1989).
- [72] N. Kidonakis and G. F. Sterman, Subleading logarithms in QCD hard scattering, *Phys. Lett. B* **387**, 867 (1996).
- [73] S. Keppeler and M. Sjö Dahl, Orthogonal multiplet bases in  $SU(N_c)$  color space, *J. High Energy Phys.* **09** (2012) 124.
- [74] Their full forms are provided in the Supplemental Material [75].
- [75] See Supplemental Material at <http://link.aps.org/supplemental/10.1103/PhysRevLett.131.211901> for the color bases that are used for the results. In these bases it also provides the soft anomalous dimension matrices before applying the absolute mass threshold limit for the  $qq$  and  $gg$  initiated processes.
- [76] S. Catani, M. L. Mangano, P. Nason, and L. Trentadue, The resummation of soft gluons in hadronic collisions, *Nucl. Phys.* **B478**, 273 (1996).
- [77] S. Forte, G. Ridolfi, J. Rojo, and M. Ubiali, Borel resummation of soft gluon radiation and higher twists, *Phys. Lett. B* **635**, 313 (2006).
- [78] A. Manohar, P. Nason, G. P. Salam, and G. Zanderighi, How bright is the proton? A precise determination of the photon parton distribution function, *Phys. Rev. Lett.* **117**, 242002 (2016).
- [79] A. V. Manohar, P. Nason, G. P. Salam, and G. Zanderighi, The photon content of the proton, *J. High Energy Phys.* **12** (2017) 046.
- [80] J. Butterworth *et al.*, PDF4LHC recommendations for LHC Run II, *J. Phys. G* **43**, 023001 (2016).
- [81] R. D. Ball *et al.* (NNPDF Collaboration), Parton distributions for the LHC Run II, *J. High Energy Phys.* **04** (2015) 040.
- [82] L. A. Harland-Lang, A. D. Martin, P. Motylinski, and R. S. Thorne, Parton distributions in the LHC era: MMHT 2014 PDFs, *Eur. Phys. J. C* **75**, 204 (2015).
- [83] S. Dulat, T.-J. Hou, J. Gao, M. Guzzi, J. Huston, P. Nadolsky, J. Pumplin, C. Schmidt, D. Stump, and C. P. Yuan, New parton distribution functions from a global analysis of quantum chromodynamics, *Phys. Rev. D* **93**, 033006 (2016).
- [84] M. van Beekveld, A. Kulesza, and L. Moreno Valero (to be published).
- [85] In the notation of Ref. [28], we include terms up to  $(N)LO_3$ .
- [86] The difference between the two lines comes, for example, from the approximation of the soft AD matrix in the absolute-threshold limit, leading to missing kinematic contributions, and not including terms that go as  $\mathcal{O}(1/N)$  or higher in the gluon emission contribution.
- [87] These differences arise from a subset of subleading terms. The treatment of subleading terms will in general differ depending on the approach chosen to invert the Mellin space result.